Diakoptic Surface Integral-Equation Formulation Applied to 3-D Scattering Problems

Dragan I. Olcan [1], Ivica M. Stevanovic [2], Branko M. Kolundzija [1], Juan R. Mosig [3], and Antonije R. Djordjevic [1]

[1] University of Belgrade, School of Electrical Engineering, 11120 Belgrade, Serbia
olcan@etf.bg.ac.yu, kol@etf.bg.ac.yu, edjordja@etf.bg.ac.yu

[2] Freescale Semiconductor, Rue de Lyon 111, CH-1211 Geneva, Switzerland
Ivica.Stevanovic@freescale.com

[3] Ecole Polytechnique Federale de Lausanne (EPFL), CH-1015 Lausanne, Switzerland
juan.mosig@epfl.ch

Abstract: The diakoptic surface integral-equation formulation (DSIE) is used for simulations of complex 3-D scatterers. Comparisons to solutions found using the classical method of moments are presented, illustrating accuracy, acceleration, and storage reduction achieved using the diakoptic approach. The implemented DSIE uses the WIPL-D engine for calculation of MoM-SIE coefficients and for the post-processing of results.

Keywords: Diakoptics, method of moments, surface integral-equation formulation, 3-D scatterers, and WIPL-D.

1. Introduction

The surface integral-equation (SIE) formulation has been used for more than a half of a century to solve electromagnetic (EM) field problems [1]-[4]. However, for complex problems, the simulations based on the SIE become unacceptably demanding in both the computer CPU time and memory resources. Hence, various approaches have been suggested to increase the efficiency of the SIE formulation [5]-[9]. We present here a general approach that can be seamlessly integrated into existing SIE codes, which we refer to as the diakoptic SIE (DSIE) formulation. In our previous work, the DSIE has been successfully applied to 2-D static and dynamic EM problems [10] and 3-D static problems [11]. In the present paper, the diakoptic approach is specialized to the dynamic analysis of 3-D metallic scatterers. In all examples, rooftop basis functions along with the Galerkin testing procedure are implemented utilizing the WIPL-D engine [12].

2. Outline of Diakoptic Surface Integral-Equation Formulation

We consider an arbitrarily shaped metallic scatterer located in a vacuum. The DSIE formulation (as well as the classical MoM-SIE) is based on the surface equivalence principle [1]. In the DSIE formulation, the original system is split into several non-overlapping subsystems. Each subsystem is encapsulated by a diakoptic (boundary) surface that acts as an interface between the subsystem and the rest of the system. For each subsystem, the unknowns are the coefficients of the surface electric current expansions on the scatterer surface and the coefficients of the equivalent surface sources on the diakoptic boundary. For the scatterer surface in a subsystem, we formulate the same SIEs as in the classic MoM-SIE approach. For the diakoptic surface, we formulate an additional SIE by requiring that the electric and magnetic fields are zero just outside the diakoptic boundary. The solution of such SIEs gives a matrix relation between the coefficients of the equivalent surface sources and the coefficients of current expansions on the scatterer surface. In order to solve the whole original system, we combine the matrix relations for all subsystems into a global diakoptic system of linear equations. Solutions of that system are the expansion coefficients of the equivalent sources at the diakoptic boundary. By using that solution and matrix relations for subsystems, the coefficients of the current expansions on the scatterer surface can be calculated. If the number of unknown coefficients for the equivalent sources at a diakoptic boundary is sufficiently smaller than the number of coefficients for the currents at the scatterer surface, DSIE solves the problems more efficiently than MoM-SIE.

3. Illustration of DSIE

The aim of this example is to illustrate the basic idea of DSIE and the influence of modeling of a diakoptic boundary to the accuracy of the final solution.

The considered scatterer is a metallic square plate, shown in Fig. 1a. The plate side is $5\,\mathrm{mm}$. The illuminating electromagnetic wave arrives from the direction perpendicular to the plane in which the scatterer resides, i.e., the direction of the incident wave is $\Phi = 0$, $\Theta = 90^\circ$ and the plate is parallel to the Oyz plane of the Cartesian coordinate system. The rms value of the incident electric field is $E = 1\,\mathrm{V/m}$ and the electric field vector is parallel to the z-axis. The frequency of the incident EM wave is $f = 3\,\mathrm{GHz}$, i.e., the electrical length of the scatterer side is $\lambda / 20$, where λ is the free-space wavelength at the operating frequency.

For the diakoptic analysis, the scatterer is wrapped with a diakoptic boundary surface. The diakoptic boundary is a cube of a side $a = 10\,\mathrm{mm}$, positioned around the scatterer, as shown in Fig. 1b. The sides of the cube are parallel to the principal planes of the Cartesian coordinate system, while the center of the cube coincides with the center of the scatterer. The original EM system is split into two diakoptic subsystems. The first diakoptic subsystem consists of the scatterer and the diakoptic boundary (Fig. 1b). The second diakoptic subsystem consists of the outer space and the same diakoptic boundary (Fig. 1c). The union of both subsystems is the whole region where the EM field exists.

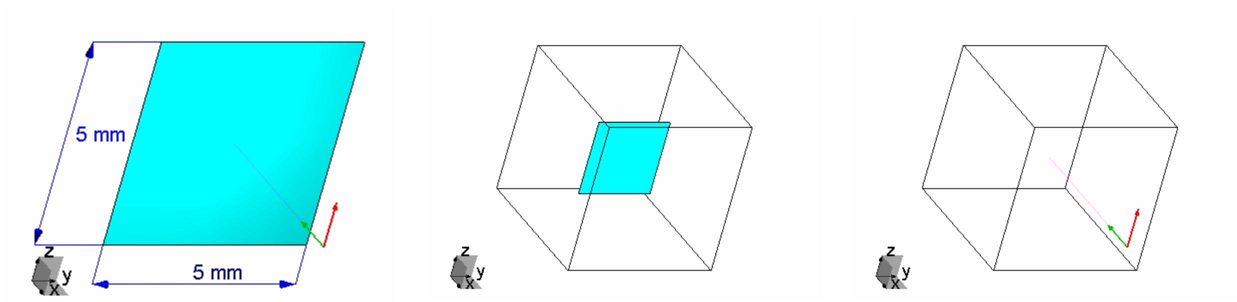

(a) Square metallic scatterer. (b) First diakoptic subsystem. (c) Second diakoptic subsystem.

Fig. 1. Square metallic scatterer and the diakoptic subsystems.

The total number of coefficients for the expansion of the electric currents on the scatterer surface is $N = 4$. The total number of coefficients for the expansion of the equivalent electric currents on the diakoptic boundary is $D = 12$ (the total number of coefficients for the equivalent magnetic currents is D, too).

Both subsystems are simulated using classical MoM-SIE to find their matrix representations. The combination of these matrices yields a diakoptic system of linear equations. The solutions of that system are the coefficients of equivalent electric and magnetic currents on the diakoptic boundary. From that solution, the coefficients for the expansion of the electric current on the scatterer surface are calculated.

First, we explore the stability of the diakoptic system of linear equations. It is essential that this system of linear equations is stable in order to get accurate results for the equivalent sources, since all other results (such as RCS, near and far fields) are calculated using these equivalent sources. We increased the numerical accuracy with which the integrals in the MoM matrix entries are computed [12] and observed the magnitude of the electric current (Fig. 2) in the direction of the incident electric field at the scatterer (z-coordinate). The RCS for the direction $\Phi = 0$ as a function of the angle Θ and the same integral accuracies as parameters is shown in Fig. 3. From Figs. 2 and 3 it is seen that there exists a slight discrepancy between the MoM-SIE and the diakoptic solution only for the lowest integral accuracy. Even that discrepancy is on the order of several percent.

Further, we explore the influence of the number of coefficients for equivalent electric (and magnetic) currents on the diakoptic boundary. The diakoptic boundary is additionally meshed into smaller quadrilaterals to increase the total number of coefficients for equivalent sources (D). The integral accuracy is set to 0 (normal) [12]. The magnitude of the electric current for various D, in the same direction as in the previous case, is shown in Fig. 4.

The RCS for various D is shown in Fig. 5. From Figs. 4 and 5 it is seen that increasing the total number of coefficients for the expansion of the equivalent sources on the diakoptic boundary enhances the accuracy of the diakoptic solution. This can be explained by the fact that by increasing D we increase the amount of information about the subsystem that is visible to other subsystems through the diakoptic boundary.

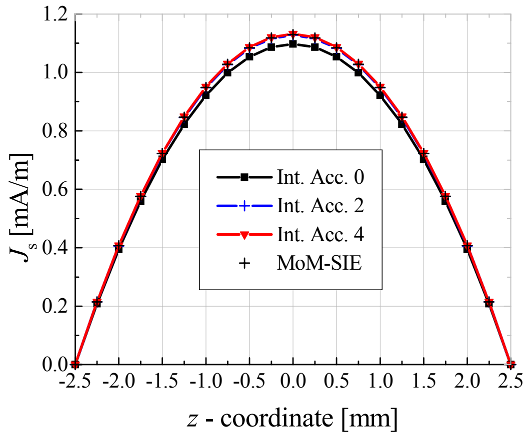

Fig. 2. Scatterer current for various integral accuracies.

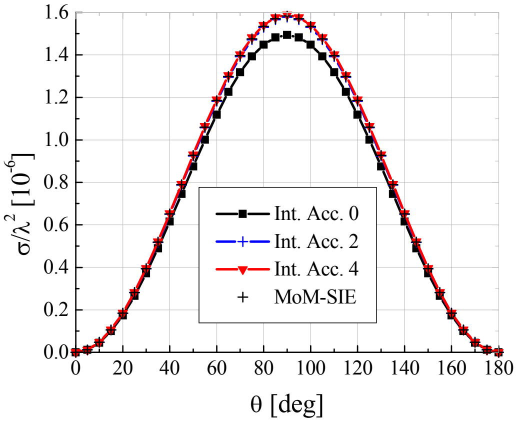

Fig. 3. RCS for various integral accuracies.

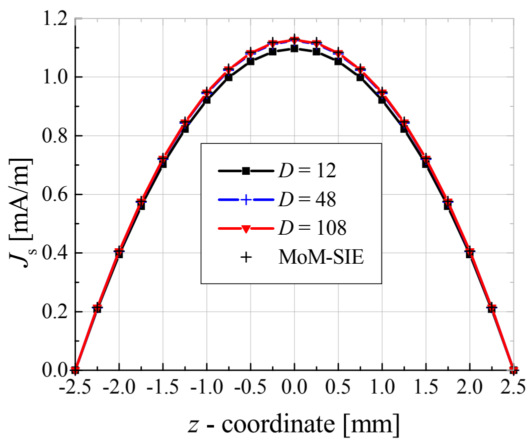

Fig. 4. Scatterer current for various number of coefficients for equivalent sources.

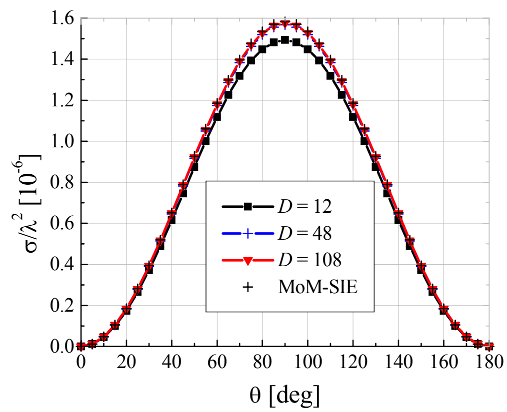

Fig. 5. RCS for various number of coefficients for equivalent sources.

Finally, we increase the frequency in order to show that the diakoptic approach can be applied for an arbitrary frequency. The new frequency is $f = 30\,\text{GHz}$. Hence, the electrical length of the plate side is $\lambda/2$ and the corresponding electrical dimensions of the diakoptic boundary are $\lambda \times \lambda \times \lambda$. The number of coefficients for equivalent electric (magnetic) currents is increased to $D = 768$ so that the rooftop basis functions can effectively approximate the equivalent sources.

The near field distribution in the vicinity of the scatterer, shown in Fig. 6, is calculated: (a) with the classical MoM-SIE approach, (b) with DSIE, (c) using equivalent sources on the diakoptic boundary and the electric currents on the scatterer surface in the first subsystem, and (d) using equivalent sources on the diakoptic boundary of the second subsystem. From Figs. 6c and 6d it is seen that the EM field is preserved inside each subsystem, while it is annihilated outside the subsystem (diakoptic) boundary, which is in accord with the applied equivalence theorem.

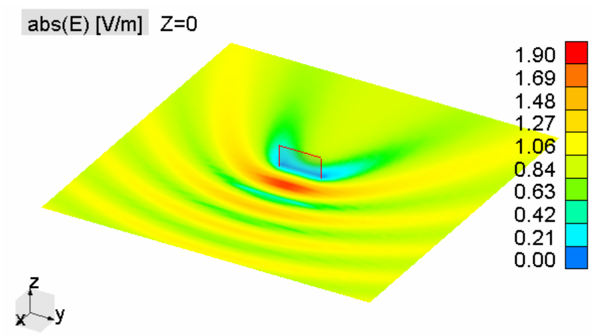

(a) MoM-SIE solution.

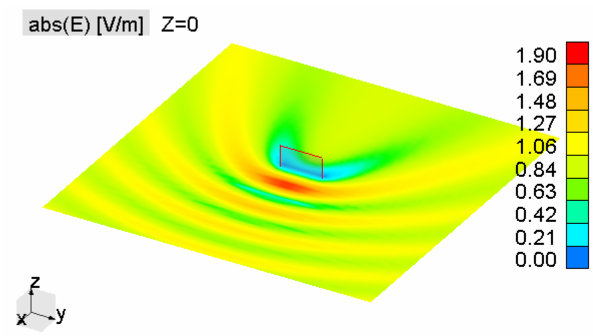

(b) DSIE solution.

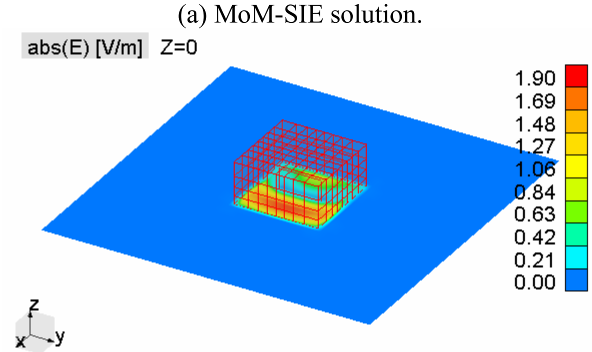

(c) First subsystem.

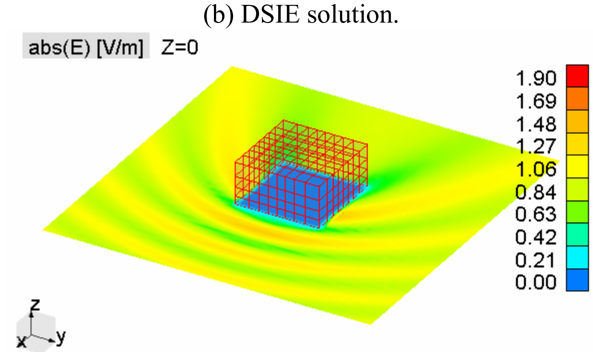

(d) Second subsystem.

Fig. 6. Near field in the vicinity of the scatterer for $f = 30\,\text{GHz}$.

The RCS for $f = 30\,\text{GHz}$, shown in Fig. 7, is calculated: (a) with the classical MoM-SIE approach, (b) with DSIE, and (c) using equivalent sources on the diakoptic boundary of the second subsystem. The results shown in Figs. 6 and 7 demonstrate that the DSIE can be used for an arbitrary frequency.

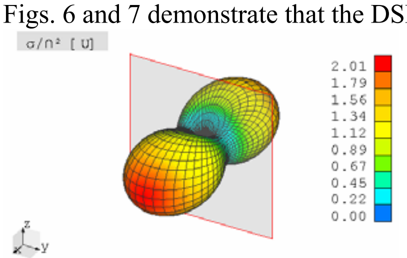

(a) MoM-SIE.

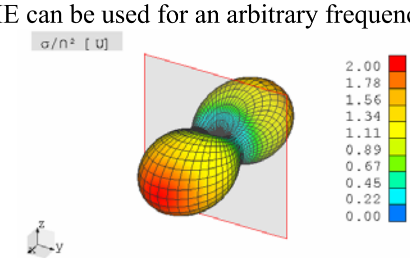

(b) DSIE.

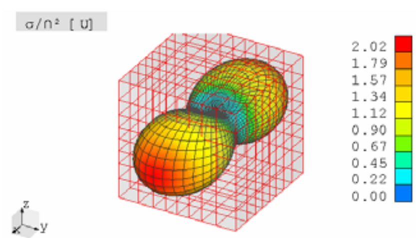

(c) DSIE equivalent sources.

Fig. 7. RCS at $f = 30\,\text{GHz}$.

Note that in this particular example, the DSIE formulation is not advantageous compared to the classical MoM-SIE as we use more unknown coefficients for the equivalent sources than the number of coefficients for the currents on the plate (scatterer).

4. Efficiency of DSIE: Scattering from Complex Structures

The aim of this example is to demonstrate the efficiency that can be achieved using DSIE, particularly the acceleration and the storage reduction when compared to the classical MoM-SIE solution.

The considered scatterer consists of 1250 identical metallic cubes grouped in 10 clusters, as shown in Fig. 8a. Each cluster consists of 125 ($5\times5\times5$) metallic cubes (Fig. 8b). The side of a cube is $a = 1\,\text{mm}$. The distance between neighboring cubes in a cluster is $d = 1\,\text{mm}$ in the x, y, and z-direction. The distance between neighboring clusters is $p = 6\,\text{mm}$ in the y and z-direction. The illuminating EM wave impinges from the direction $\Phi = 0$, $\Theta = 90^\circ$. The rms value of the incident electric field is $E = 1\,\text{V/m}$ and the electric field vector is parallel to the z-axis. The frequency of the incident EM wave is $f = 15\,\text{GHz}$. The electrical length of the cube side is $\lambda/20$. The dimensions of one cluster are $9\lambda/20\times9\lambda/20\times9\lambda/20$ and the dimensions of the whole scatterer are

$3.5\lambda \times 1.25\lambda \times 9\lambda / 20$. The total number of the unknown coefficients for the electric current expansions for the whole scatterer is $N_{\mathrm{tot}} = 15\,000$, i.e., 12 per metallic cube.

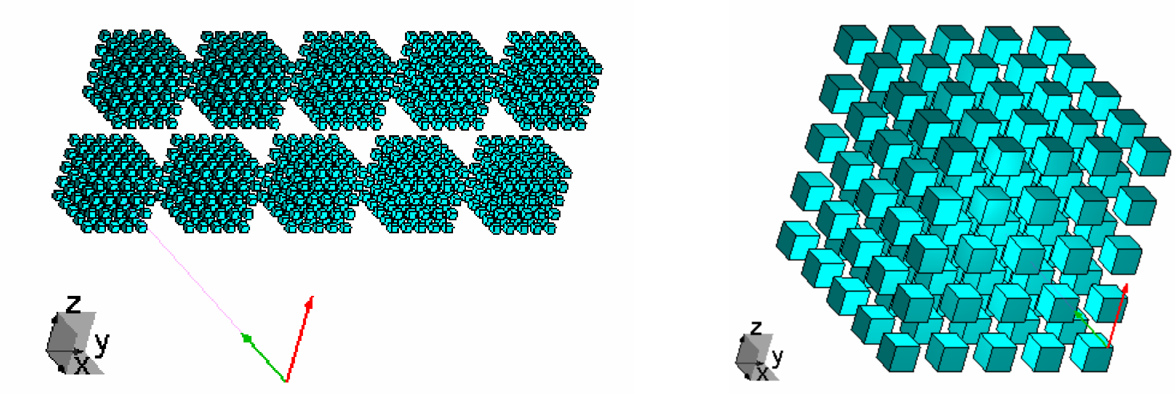

(a) Complex scatterer. (b) One cluster of cubes.

Fig. 8. The complex scatterer.

For the diakoptic approach, the scatterer is divided into 11 subsystems. The first one consists of the outer space and the diakoptic boundaries of the other 10 subsystems (Fig. 9a). The remaining 10 subsystems are congruent. Each of them consists of a cluster of 125 cubes wrapped with a diakoptic boundary (Fig. 9b). The diakoptic boundary is a cube of a side $b = 11\,\mathrm{mm}$. The total number of the unknown coefficients for the current expansions of the equivalent electric (magnetic) currents on the diakoptic boundary is $D = 192$ and for the encapsulated cluster is $N = 1500$. Since we have 10 congruent systems, their diakoptic matrices are identical and, therefore, we solve only two subsystems with MoM-SIE: the first one and one of the remaining 10 congruent subsystems.

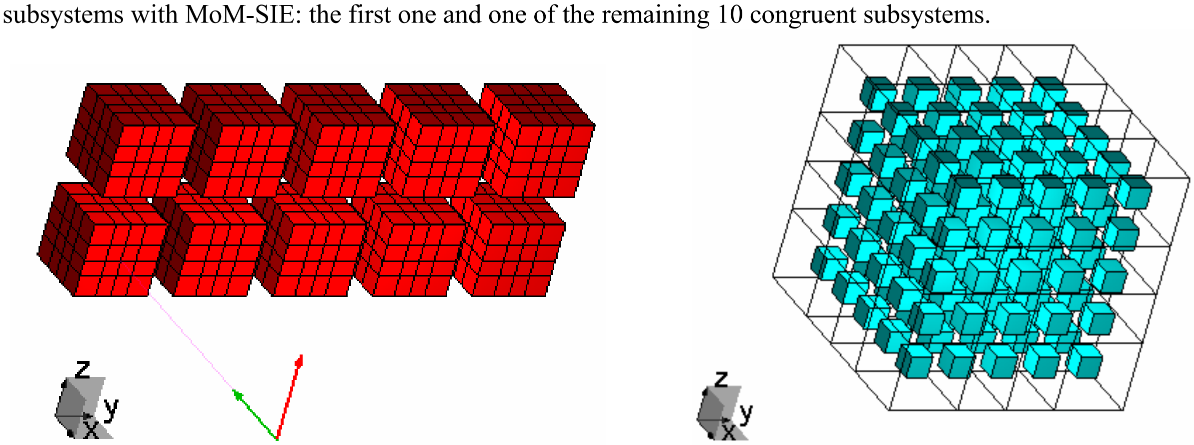

(a) The first subsystem. (b) One of 10 congruent subsystems.

Fig. 9. Subsystems for the diakoptic approach.

The RCS calculated with the classical MoM-SIE and the DSIE formulations is shown in Fig. 10 for two cuts (a) $\Theta = 88^\circ$ and (b) $\Phi = 180^\circ$. The results calculated using DSIE and MoM-SIE match very well.

The acceleration of DSIE approach can be calculated as $a = t_{\mathrm{SIE}} / t_{\mathrm{DSIE}}$, where t is the time needed for each of these simulations. The simulation of the whole scatterer at once using WIPL-D [12] out-of-core solver takes $t_{\mathrm{SIE}} = 24\,557\,\mathrm{s}$ on a 32-bit desktop PC with 512 MB of RAM. On the same PC, the DSIE simulation takes only $t_{\mathrm{DSIE}} = 619\,\mathrm{s}$. Therefore, the achieved acceleration is $a = 39.7$. Theoretically, the maximal acceleration that can be achieved in this example is $a = \dfrac{(KN)^3}{2(KD)^3 + (N+D)^3} = 177.6$, if the inversion of matrices ($\sim O(N^3)$) is the dominant time-consuming process.

The storage reduction of the DSIE approach can be calculated as $m = s_{\mathrm{SIE}} / s_{\mathrm{DSIE}}$, where s is the memory (RAM) used for each of these simulations. To store the MoM-SIE matrix of the whole scatterer (double precision complex numbers), it takes $s_{\text{SIE}} = 3.6\,\text{GB}$. The largest matrix that is stored in the DSIE approach is the MoM matrix for the first subsystem that consists of 1920 coefficients and it takes $s_{\text{DSIE}} = 59\,\text{MB}$. Two such matrices are needed during the DSIE simulation. Therefore, the achieved storage reduction in this example is $m \approx 30.5$.

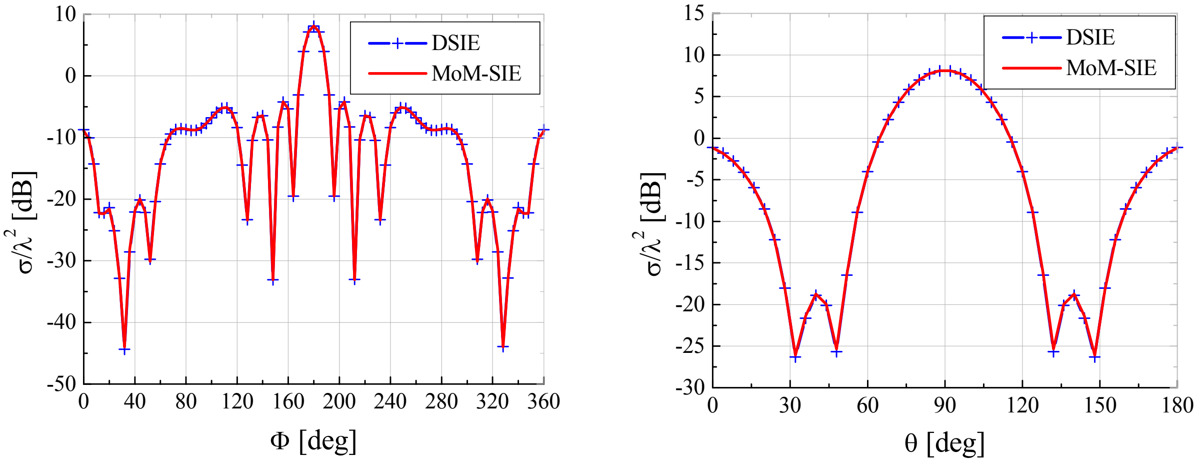

(a) Θ -cut. (b) Φ -cut.

Fig. 10. RCS calculated using DSIE vs. classical MoM-SIE.

5. Conclusions

In this paper we have shown that the diakoptic surface integral-equation (DSIE) formulation can be efficiently used for the simulations of complex 3-D scatterers. Significant accelerations and storage reductions, compared to the classical MoM-SIE formulation, are achieved without compromising the accuracy of the final results.

The future work will include composite metallic and dielectric structures, antennas, higher-order basis functions, and optimization-for-speed of the diakoptic code.

References

[1] R.F. Harrington, *Time-Harmonic Electromagnetic Fields*, New York: McGraw-Hill Book Company, 1961.

[2] R.F. Harrington, *Field Computation by Moment Methods*, New York: Macmillan, 1968. Reprinted by IEEE Press, 1993.

[3] J.R. Mosig, "Integral-equation technique," in *Numerical Techniques for Microwave and Millimeter-Wave Passive Structures,* T. Itoh, ch. 3, pp. 133-213, Ed. New York: Wiley, 1989.

[4] B.M. Kolundzija and A.R. Djordjevic, *Electromagnetic modeling of composite metallic and dielectric structures*, Boston: Artech House, 2002.

[5] R. Coifman, V. Rokhlin, and S. Wandzura, "The fast multipole method for the wave equation: a pedestrian prescription," *IEEE Antennas and Propagation Magazine*, Vol. 35, No. 3, pp. 7-12, June 1993.

[6] W.C. Chew, J. Jin, C. Lu, E. Michielssen, and J.M. Song, "Fast solution methods in electromagnetics," *IEEE Transactions on Antennas and Propagation*, Vol. 45, No. 3, pp. 533-543, October 1997.

[7] J. Rius, J. Parron, E. Ubeda, and J.R. Mosig, "MLMDA for analysis of electrically large electromagnetic problems in 3D," *Microwave Opt. Technol. Lett*., vol. 22, no. 3, pp. 178–182, Aug. 1999.

[8] B. Stupfel and M. Mognot, "A domain decomposition method for the vector wave equation," *IEEE Transactions on Antennas and Propagation*, Vol. 48, No. 5, pp. 653-660, May 2000.

[9] M. Li and W.C. Chew, "Wave-field interaction with complex structures using equivalence principle algorithm," *IEEE Transactions on Antennas and Propagation*, Vol. 55, No. 1, pp. 130-138, January 2007.

[10] D.I. Olcan, I.M. Stevanovic, J.R. Mosig, and A.R. Djordjevic "Diakoptic approach to analysis of multiconductor transmission lines," accepted for publication in *Microwave Opt. Technol. Lett*. in April 2008.

[11] D.I. Olcan, I.M. Stevanovic, J.R. Mosig, and A.R. Djordjevic, "Diakoptic surface integral equation formulation applied to 3-D electrostatic problems," *Proc. of ACES 2007*, Verona, Italy, pp. 492-498, March 2007.

[12] WIPL-D Pro v6.4, "Software and User's Manual," WIPL-D d.o.o., Belgrade, 2007, www.wipl-d.com